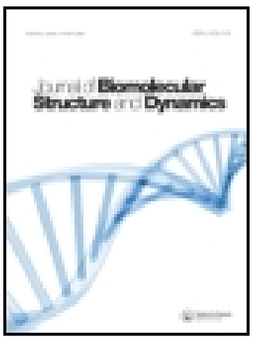

Taylor & Francis
Taylor & Francis Group

Journal of Biomolecular Structure and Dynamics

ISSN: 0739-1102 (Print) 1538-0254 (Online) Journal homepage: https://www.tandfonline.com/loi/tbsd20

New strategy for identifying potential natural HIV-1 non-nucleoside reverse transcriptase inhibitors against drug-resistance: an *in silico* study

Yanjing Wang, Xiangeng Wang, Yi Xiong, Aman Chandra Kaushik, Junaid Muhammad, Abbas Khan, Hao Dai & Dong-Qing Wei

To cite this article: Yanjing Wang, Xiangeng Wang, Yi Xiong, Aman Chandra Kaushik, Junaid Muhammad, Abbas Khan, Hao Dai & Dong-Qing Wei (2019): New strategy for identifying potential natural HIV-1 non-nucleoside reverse transcriptase inhibitors against drug-resistance: an *in silico* study, Journal of Biomolecular Structure and Dynamics, DOI: 10.1080/07391102.2019.1656673

To link to this article: https://doi.org/10.1080/07391102.2019.1656673

JOURNAL OF BIOMOLECULAR STRUCTURE AND DYNAMICS
https://doi.org/10.1080/07391102.2019.1656673

New strategy for identifying potential natural HIV-1 non-nucleoside reverse transcriptase inhibitors against drug-resistance: an *in silico* study

Yanjing Wang[a,b], Xiangeng Wang[a,b], Yi Xiong[a], Aman Chandra Kaushik[a], Junaid Muhammad[a], Abbas Khan[a], Hao Dai[c] and Dong-Qing Wei[a]

[a]State Key Laboratory of Microbial Metabolism, School of Life Sciences and Biotechnology, and Joint Laboratory of International Cooperation in Metabolic and Developmental Sciences, Ministry of Education, Shanghai Jiao Tong University, Shanghai, China; [b]Peng Cheng Laboratory, Nanshan District, Shenzhen, Guangdong, China; [c]Shanghai Institute of Biochemistry and Cell Biology, Chinese Academy of Sciences, Shanghai, China

Communicated by Ramaswamy H. Sarma.

ABSTRACT

Non-nucleosides reverse transcriptase inhibitors (NNRTIs), specifically targeting the HIV-1 reverse transcriptase (RT), play a unique role in anti-AIDS agents due to their high antiviral potency, structural diversity, and low toxicity in antiretroviral combination therapies used to treat HIV. However, due to the emergence of new drug-resistant strains, the development of novel NNRTIs with adequate potency, improved resistance profiles and less toxicity is highly required. In this work, a novel virtual screening strategy combined with structure-based drug design was proposed to discover the potential inhibitors against drug-resistant HIV strains. Seven structure-variant RTs, ranging from the wild type to a hypothetical multi-mutant were regarded as target proteins to perform structure-based virtual screening. Totally 23 small molecules with good binding affinity were identified from the Traditional Chinese Medicine database (TCM) as potential NNRTIs candidates. Among these hits, (+)-Hinokinin has confirmed anti-HIV activity, and some hits are structurally identical with anti-HIV compounds. Almost all these hits are consistent with external experimental results. Molecular simulations analysis revealed that top 2 hits (Pallidisetin A and Pallidisetin B) bind stably and in high affinity to HIV-RT, which are ready to be experimental confirmed. These results suggested that the strategy we proposed is feasible, trustworthy and effective. Our finding might be helpful in the identification of novel NNRTIs against drug-resistant, and also provide a new clue for the discovery of HIV drugs in natural products.

ARTICLE HISTORY
Received 16 October 2018
Accepted 8 August 2019

KEYWORDS
Reverse transcriptase; NNRTIs; virtual screening; TCM; HIV

1. Introduction

The first case of Acquired Immune Deficiency Syndrome (AIDS) has been reported since 1981 (Gottlieb et al., 1981). As a serious threat to global health (Zhou, Ning, Lee, Hambly, & McLachlan, 2016), the development of the specific inhibitors against human immunodeficiency virus (HIV) replication to reduce the viral infection is still a leading treatment strategy against HIV/AIDS (Broder, 2010). Reverse transcriptase (RT) of HIV, has been considered as one of the most promising targets for anti-HIV treatment and numerous approved RT inhibitors that are critical components of antiretroviral combination therapies (cART) (Shafer & Vuitton, 1999).

Based on the binding site and chemical class of compounds, RT inhibitors are classified into nucleoside RT inhibitors (NRTIs) and non-nucleoside RT inhibitors (NNRTIs). Compared to NRTIs, NNRTIs are advantageous of potent antiviral activity, high selectivity, low toxicity, and specificity(de Bethune, 2010). In all the reported structures of NNRTI-RT complex, the inhibitor binds to a hydrophobic pocket (non-nucleoside inhibitor binding pocket, NNIBP) located in the junction of the palm and thumb subdomain of HIV- RT protein(Sarafianos, Das, Hughes, & Arnold, 2004) (Figure 1). The pocket distal to the active site within RT is formed by β6-β10-β9 and β12-β13-β14 sheets of the p66 subunit (Figure 2(A)). The presence of NNRTI will induce allosteric rearrangements, interfering the binding capacity of the enzyme with nucleotide substrate and will consequently impair the associated DNA synthesis in virus (Squires, 2001). Moreover, the inherent flexibility of NNIBP results in both structural and chemical diversity of NNRTIs, providing opportunities for novel scaffold discovery (Hsiou et al., 1996; Bauman et al., 2008).

Currently, more than 50 structurally diverse classes of compounds have been reported as NNRTIs (Zhan et al., 2013; Li et al., 2014; Sluis-Cremer, 2018). There are six NNRTIs (Figure S1, Supporting Material) approved for clinical use: nevirapine (NVP, 1996), delavirdine (DLV, 1997), efavirenz (EFV, 1998), etravirine (ETR, 2008), rilpivirine (RPV, 2011), and doravirine (DOR, 2018) (Namasivayam et al., 2019).

CONTACT Dong-Qing Wei dqwei@sjtu.edu.cn; Hao Dai wys8c764@126.com
Supplemental data for this article is available online at https://doi.org/10.1080/07391102.2019.1656673.

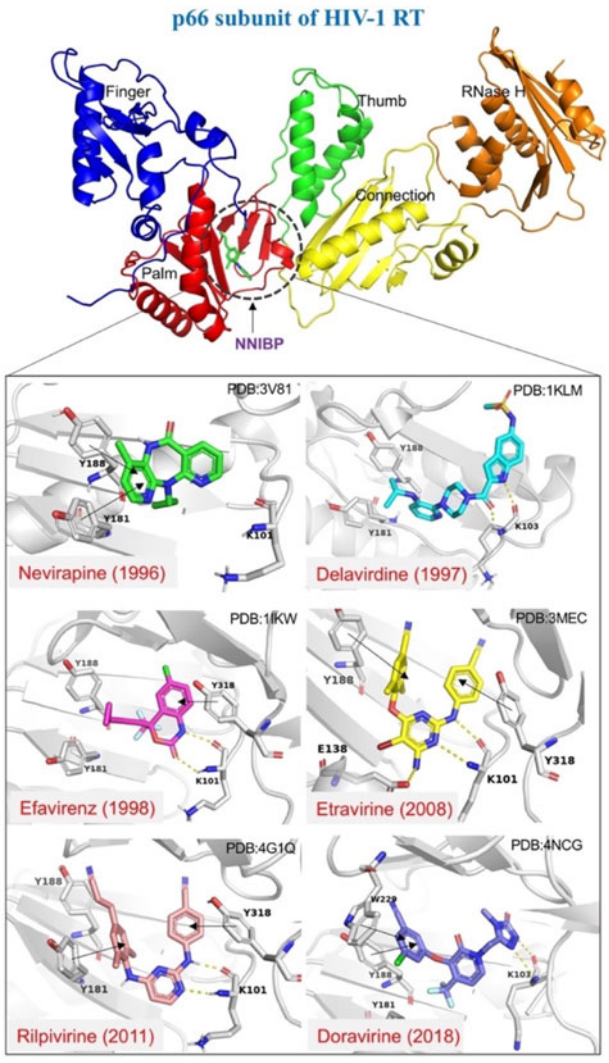

Figure 1. Ribbon representation of HIV-1 RT protein (p66 subunit, chain A) complexes with marketed NNRTIs. Five subdomains of p66 subunit (fingers, palm, thumb, connection, and RNase H) are shown in blue, red, green, yellow, and orange, respectively. A close-up view in box of NNIBP (NNRTI binding pocket), nearby regions and the binding with Nevirapine, Delavirdine, Efavirenz, Etravirine, Rilpivirine, and Doravirine. These drugs are in stick representation.

Commonly, the HIV strains can variably escape the selective pressure via error-prone replication and result in the dominance of new resistant RT variants(Preston, Poiesz, & Loeb, 1988; Roberts, Bebenek, & Kunkel, 1988). Despite the chemical diversity of NNRTIs, the antiviral potency of most clinical NNRTIs was impaired in varying degrees by resistance-associated mutations in the binding pocket (Menendez-Arias, 2013; Wensing et al., 2015). The most frequent mutations, such as L101I, K103N, V106A, Y181C, and Y188L, which can appear alone or in combination. Moreover, the cross-resistance among NNRTIs has appeared frequently (Delaugerre et al., 2001; Sluis-Cremer & Tachedjian, 2008; Sluis-Cremer, 2014). Therefore, it is imperative to continually develop new NNRTIs with high potency and improved drug-resistance profiles(Zhan, Pannecouque, De Clercq, & Liu, 2016). The first-generation NNRTIs (NVP, DLV) possess rigid structures and adopt a "butterfly-like" conformation in NNIBP. The second-generation (EFV) and third-generation (ETR, RPV, DOR) exhibit more flexible "horseshoe-like" model which can establish a crucial hydrogen bond interaction with nonhydrophobic residues including K103, K101, and P236 (Figure 1). Such adaptations of pharmacophore model and drug binding interaction are critical for designing the next generation of NNRTIs with a wide range of drug-resistant HIV-1 RTs (Battini & Bollini, 2019).

Natural products, exhibiting a wide range of pharmacophores, a high degree of stereochemistry, is a promising source of antiviral agents (Koch et al., 2005). Several compounds of specific chemical classes (such as coumarins, alkaloids, phenolics, lignans, and flavonoids) isolated from medicinal plants have been reported to show anti-HIV activity (Singh, Bharate, & Bhutani, 2005; Kurapati, Atluri, Samikkannu, Garcia, & Nair, 2016; Salehi et al., 2018), as well as several natural molecules, have been extensively studied as effective NNRTIs to treat drug-resistant HIV-1 (Creagh et al., 2001; Acuna, Jancovski, & Kennelly, 2009; Li, Hattori, & Kodama, 2011). The computer-aided drug design (CADD) method, supported by known inhibitors and structural biology studies(De Clercq, 2002), has also successfully helped us to propose new potential NNRTIs(Ragno et al., 2004; Janssen et al., 2005; Jorgensen et al., 2006; Lu et al., 2012; Santos, Ferreira, & Caffarena, 2015).

To find news hits and even new NNRTI scaffolds for HIV-1 RT, we proposed a new structure-based virtual screening (VS) strategy inspired by biological evolution (Andersson & Levin, 1999; Palumbi, 2001). We selected the TCM Database @Taiwan (Chen, 2011) as the major data source and we found 23 promising hits by a series of screening procedures. Among them, two cinnamoyl bibenzyls, Pallidisetin A and Pallidisetin B, investigated in detail utilizing molecular dynamics simulations, exhibited better binding affinity to both wild-type and drug-resistance HIV variants than some marketed drugs. The strategy used in this work provides a feasible approach to discover the potential scaffolds of HIV-1 RT inhibitors. Figure 3 illustrates a flowchart of the present study with the various phases of the computational methods.

2. Materials and methods

2.1. Structural alignment of RT mutants

To identify variations in the structures of RT, we retrieved ten RT wild and mutant structures (Table S5, Supporting material) complexed with different NNRTIs from Protein Data Bank (http://www.rcsb.org). Structural alignment was performed via MODELLER/Align3D in Discovery Studio 3.1 (Accelrys Co., Ltd., US) with the default parameters. Structural alignment is a useful way to obtain important information about the secondary structure, conserved residues and the binding site. The tertiary structure of the binding pocket residues (Val90 to Gly112, Asn175 to Glu194, His221 to Thr240 of P66 subunit) in different mutants were also obtained via structural alignment.

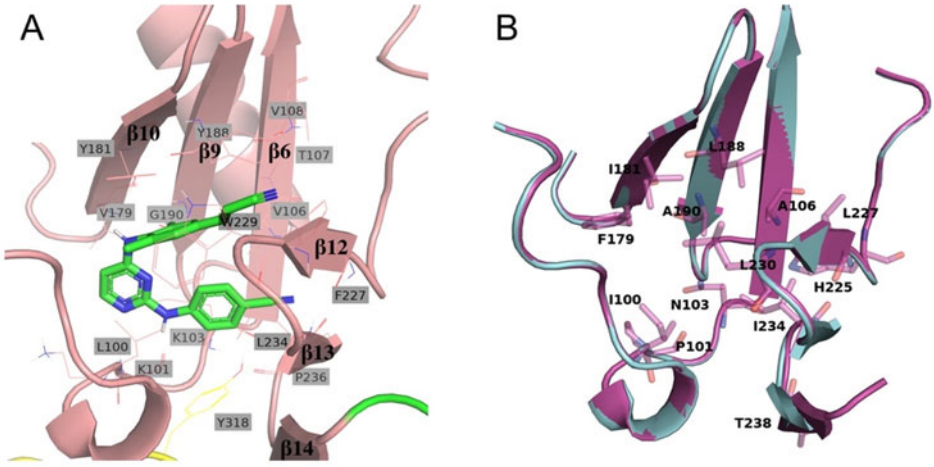

Figure 2. Binding pocket and structure alignment. (A) The hydrophobic NNRTIs binding pocket (NNIBP) of WT-RT. This pocket includes some hydrophobic amino acids (L100, V106, T107, V108, V179, Y181, Y188, G190, F227, W229, L234, and Y318) and a few nonhydrophobic residues (K103, K101, and P236) (B) The structure alignment of hypothetical multi-mutant structure (HM) and template structure (HIV-1 RT). HM was shown in purple cartoon and template structure is shown in cyan. The 13 NNRTI resistance mutations were marked by stick.

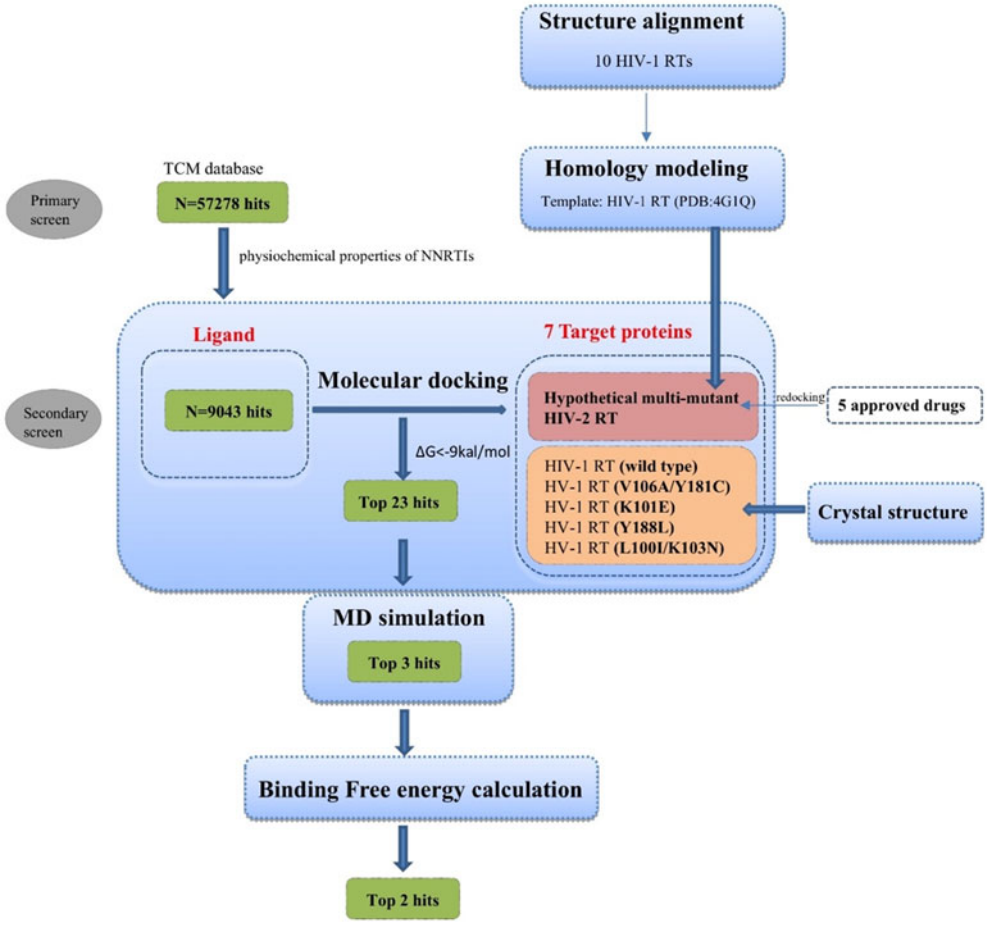

Figure 3. The workflow of this study.

2.2. Homology modeling

In this study a hypothetical multi-mutant (HM) RT protein including mutation L100I, K101P, K103N, V106A, V179F, Y181I, Y188L, G190A, P225H, F227L, M230L, L234I, and K238T simultaneously was use as one of target protein for virtual screening. These 13 mutations are common NNRTI resistance mutations in NNIBP (Shafer & Schapiro, 2008; Clutter, Jordan, Bertagnolio, & Shafer, 2016; Wensing et al., 2017). The sequence of HM was constructed from the wild-type HIV-1 RT sequence (SwissProt: P03366) and its structure is predicted by homology modelling with the template of HIV-1 RT (PDB ID: 4G1Q). We also consider HIV-2 RT as another target protein for virtual screening. However, the structure of HIV-2 RT complexed with NNRTI is also not available in the

protein structure databases. Thus, homology model of HIV-2 RT was also constructed from HIV-2 RT by using HIV-1 RT (PDB ID:4G1Q) as the template structure. HIV-2 RT sequence was downloaded from uniProt (https://www.uniprot.org/).

All aforementioned structures were predicted by comparative modeling using MODELLER 9.1.2 program. In the process of template modeling for each protein, 10 potential structure models were generated, and the conformation with the lowest DOPE (Discrete Optimized Protein Energy) score was used as the final predicted structure. The predicted structures were validated using the PROCHECK to evaluate backbone conformation based on Ψ/Φ of Ramachandran plot analysis in SAVES (http://servicesn.mbi.ucla.edu/SAVES/). Furthermore, the effectiveness of the two predicted structures was later evaluated by the redocking of five marketed NNRTIs (Nevirapine, Delavirdine, Efavirenz, Etravirine, Rilpivirine).

2.3. Preparation of receptor protein

The 3D structures of the seven RTs, used as receptor, were subjected to structure preparation. It is an important step before molecular docking, MD simulations to remove clashes, refine the secondary structure elements, and bonds order. Among the total seven proteins (wild and mutants), two were modeled (HM and HIV-2 RT) while the remaining five structures were obtained from the protein databank using 4G1Q (wild type, 1.5 Å), 3DMJ (V106A, Y181C), 2HND (K101E), 2YNF (Y188L) and 2ZE2 (L100I, K103N) accession numbers. Ligands and water molecules were removed from original Protein Data Bank file and all the receptors were subjected to energy minimization using the Discovery Studio 3.1. Hydrogen atoms were added and the geometry of all the hetero groups was corrected.

2.4. Ligand database of TCM

A total of 57,278 natural compounds were retrieved from different sources including 37,170 from TCM Database@Taiwan (http://tcm.cmu.edu.tw) (Chen, 2011) and 20,108 from the Chinese medicine chemistry database built by our laboratory. The initial screening was based on the physicochemical properties to fulfil the NNRTIs criteria for a suitable candidate. The calculated physiochemical properties of the existing NNRTI inhibitors are given in Table S5, Supporting material. These properties used to filter out the compiled ligands database are summarized in Table 1. This screening was carried out by using our in-house developed program SAMM (Shanghai Molecular Modeling) to filter and calculate the properties. Compounds successfully passing these criteria were subjected to the further process molecular docking.

2.5. Molecular docking

Following the protein targets and ligands database preparation, molecular docking with AutoDock Vina tools v1.5.6 was performed. For the docking process, each compound was converted into a ".pdbqt" format using Raccoon (http://autodock.scripps.edu/resources/raccoon) and further used to carry out virtual screening. Gasteiger partial charges were assigned during docking. The translation, quaternion, and torsion criteria were set as default in AutoDock. All torsions were allowed to rotate during docking. The grid box ($x = 15$ Å, $y = 15$ Å, $z = 18$ Å) for docking calculations was centered on NNIBP of receptors, enclosing the residues around the active site. Lamarckian genetic algorithm (LGA) was applied for conformational sampling. The number of docking runs was set to 10. All other parameters in the protocol were kept as default. Batch docking was performed by an inhouse written script that contains space size and coordinate of docking center. After docking, the 10 solutions for every ligand were clustered into groups with RMS deviations lower than 1.0 Å. The clusters were ranked by the lowest energy representation of each cluster. Finally, the compounds were selected with a cut off docking score value (ΔG)-9.0 kcal/mol as potential candidates against the targets. In order to evaluate our molecular docking method, we performed docking on the decoy set (Mysinger, Carchia, Irwin, & Shoichet, 2012), designed specifically for HIV-RT (http://dude.docking.org/), versus all seven targets. This set consists of 1178 structural unique chemicals which is believed to have no binding affinity to HIV-RT. The final screening hits were further evaluated via an online webserver HIVprotI (Qureshi, Rajput, Kaur, & Kumar, 2018) (http://bioinfo.imtech.res.in/manojk/hivproti), which reads the SMILES (simplified molecular input line entry system) representation of chemicals and produces predicted IC50 values for HIV-1 RT. HIVprotI platform employs support vector machine (SVM) based QSAR models trained on experimentally validated data from ChEMBL repository.

Table 1. The physiochemical criteria used for screening NNRTIs.

Parameters	Values
Molecular weight	260–500
Number of H-bond acceptors	1–7
Number of H-bond donors	0–5
Area of van der Waals surface	230–520
van der Waals volume	300–610
Octanol–water partition coefficient (LogP)	0.7–6.7
Number of rotatable bonds	1-10

2.6. Molecular dynamics (MD) simulations

Top 3 hits with high docking score were selected for MD simulation to explore the protein-ligand binding dynamic. In particular, to predict the antiresistant of the compound, top 2 hits docking against two mutant RTs were also subjected to simulation studies. Wherein, three different RT structures (PDB: 2ZE2, 2HND) were used as controls in simulation group, binding to the first and third generation NNRTIs: Nevirapine (NVP) and Rilpivirine (RPV), respectively. The details of the simulation systems in this work are summarized in Tables S8 and S9, Supporting material. The initial coordinates for the complexes were taken from optimum conformation in the docked pose (Figure 4). We considered the pose which has hydrogen-bond with hot residue position (such as 101, 103, or 236) or $\pi-\pi$ stacking interaction with some residues (such as Y188, Y181, W229). Further, only p66 subunit of chain A was selected to work for improving the calculation efficiency. All these simulations were carried out using the GROMACS V5.0 program with Charmm36 force

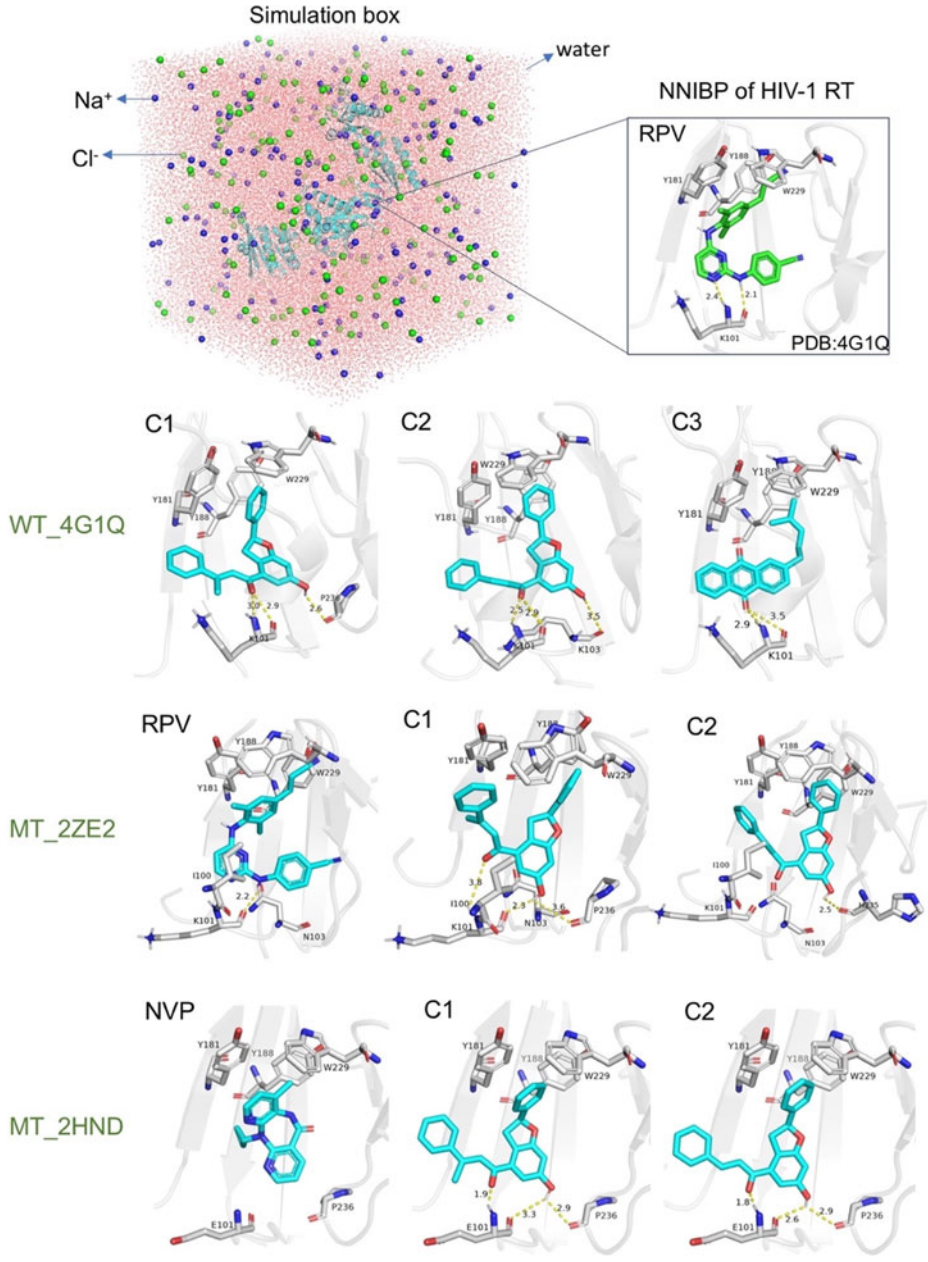

Figure 4. Initial conformation for MD simulation and schematic diagram of simulation box.

filed parameter set (Best et al., 2012). The GROMACS topologies for the ligands were obtained from the CGenFF program (https://cgenff.paramchem.org/)(Vanommeslaeghe et al., 2010). Relevant parameters were set as follows: the distance between the edge of the cubic box and complex was set at 10 Å. The resultant system was solvated, using TIP3P water models, followed by the addition of ions to neutralize the system to 0.15 M NaCl concentration. The production run was carried out for 30 ns on all the systems. At the same time, it was integrated with motion equation for NPT ensemble at 300 K and 1.01325 × 105 Pa (1 atmospheric pressure), controlled by V-rescale thermostat (Hess, Kutzner, Van Der Spoel, & Lindahl, 2008) and Parrinello-Rahman Barostat, respectively. The SHAKE algorithm was employed to constrain bond length involving hydrogen atoms to follow 2 fs step interval. Whereas, MD simulation coordinates for all the systems were saved at every 10 ps.

2.7. MD data analysis

All the analyses have been performed on 30 ns trajectories (3,000 structure) of each MD system after elimination of the rotational and translational movements. Moreover, root mean square deviation (RMSD), root mean square fluctuation (RMSF) and gyration radius (Rg) analysis have been carried out using tools implemented in the GROMACS v5.0. Also, hydrogen bonds were defined with hydrogen-acceptor at a distance less than 3.5 Å and donor-hydrogen-acceptor angle with more than 135°. Additionally, the frequency of hydrogen bonds in every trajectory was calculated by MDAnalysis package (Michaud-Agrawal, Denning, Woolf, & Beckstein, 2011) with an in-house written script. The VMD software package(Humphrey, Dalke, & Schulten, 1996) was used for visual analysis of MD trajectories. All the structures were also visualized using Pymol (www.pymol.org). Further, LigPlot+

program (Laskowski & Swindells, 2011) was employed to obtain the 2D ligand-protein interaction diagrams.

2.8. Binding free energy calculations

Binding free energy predictions were performed using molecular mechanics Poisson–Boltzmann surface area (MM-PBSA) method, implemented by a g_mmpbsa tool, that integrates functions from GROMACS and APBS (Kumari, Kumar, Open Source Drug Discovery, & Lynn, 2014). The calculation is based on the following equations,

$$\begin{cases} \Delta G_{\text{bind}} = G_{\text{complex}} - G_{\text{protein}} - G_{\text{ligand}} \\ \Delta G_{\text{bind}} = \Delta E_{\text{MM}} + \Delta G_{\text{PB}} + \Delta G_{\text{nonpolar}} - T\Delta S \\ \Delta G_{\text{bind}} = G_{\text{ele}} + G_{\text{vdw}} + G_{\text{SA}} + G_{\text{PA}} \end{cases}$$

where ΔE_{MM} is the sum of van der Waals and electrostatic energy, ΔG_{PA} is polar solvation energy; ΔG_{SA} is nonpolar solvation energy. The final, binding energy ΔG_{bind} is relative value rather than the absolute value because the vibrational entropy contribution ($T\Delta S$) was not included in our calculation. Total 1,000 snapshots at an interval of 10 ps from last 10 ns trajectories during stable phase were extracted as a sampling for calculations.

3. Results and discussion

3.1. Structural comparisons

To explore the mechanism of drug resistance and elucidate the structural differences of RT bounding to various ligands, NNIBP of 10 RT crystal structures were investigated via structure alignment. As shown in Figure S1, Supporting material, 10 structures exhibited very similar secondary structure. RMSD value of Cα atom in backbone was 0.7 to 1.9 Å and resolution of most crystal structures were in the range of 2.3 to 2.9 Å (Table S2, Supporting material). From these observations, we could conclude that there is no significant difference in main chain positions of active sites. Moreover, distribution analysis of the 13 residues around the NNRTI was shown in Figure S1B, Supporting material. The residues in the proximity of ligands (Table S3, Supporting material) were almost not conserved, and drug-resistant mutations caused by NNRTI were concentrated near the NNRTI binding region(Clutter et al., 2016). A recent study on HIV-1 RT crystal structures also revealed that the NNRTI-resistant mutant impairs the dynamics of HIV-1 RT or NNRTI binding via altering the shape of the binding pocket, rather than significantly affecting RT structure(Seckler, Leioatts, Miao, & Grossfield, 2013). Our strategy to combat drug-resistant HIV strains is to design drugs with a broad antimutation spectrum which have good binding affinities to various mutated proteins simultaneously.

3.2. Target protein modeling

A hypothetical multi-mutant was shown in Figure 2(B), harboring a wide range of 13 known drug-resistant mutants(Shafer & Schapiro, 2008; Clutter et al., 2016), was generated based on high-resolution HIV-1 RT structure (1.51 Å) (Kuroda et al., 2013). Figure 2. It is an extreme condition that a hypothetical target protein has a broad-variation spectrum. We also considered another extreme condition where the HIV species is different. This scenario is embodied by the HIV-2 RT structure. The structure alignment of modeled HIV-2 RT and HIV-1 RT are shown in Figure S3, Supporting material. Predicted structures were optimized and then validated by Ramachandran plot Figure S4, Supporting material. Our aim is to design a computational structure exhibiting high similarity with that of HIV-1 backbone but a significant difference in side chains. Moreover, the NNRTI resistance mutations of HIV-1 RT (Wensing et al., 2017; Shafer & Schapiro, 2008) and corresponding residues in HIV-2 RT were summarized in Table S3, Supporting material.

Five marketed NNRTIs docking with HIV-1 RT, HM, and HIV-2 RT to evaluate the effectiveness of the models. The docking results are summarized in Table S4, Supporting material. The docking scores were observed in an order as HIV-1 > HIV-2 > HM, indicating that the two predicted structures (HM and HIV-2 RT) have significant reduction in drug binding affinity.

3.3. Structure-based virtual screening of TCM database

The library of 57,278 natural compounds were filtered by the physiochemical criteria during the primary screening. Then, seven RT structure models (five HIV-1 RTs, HM RT, HIV-2 RT) obtained after the validation procedure were used for docking screening of 9,043 natural compounds. Finally, we identified the 23 top scored compounds according to their docking score value (against to WT RT, PDB: 4G1Q) with respect to the best pose (Table 2; Figure 5 and Figure S5, Supporting material). No chemical in decoy set has met the threshold of docking score by our docking protocol, which suggests the reliability of our docking procedure. We further analyzed the physicochemical properties of the best hits and we observed that all of them within a range of criteria we summarized from NNRTIs (Table S5, Supporting material).

The conformational properties of the 23 promising screened compounds are very intriguing, because these compounds have similar tricyclic structures (Compound 1, 2, 11, 12, 17, 18, 20, 21) as approved drugs such as Delavirdine, Etravirine, Rilpivirine (Figure S1, Supporting material). The overall similarity in binding mode of 23 hits to the RT in docking pose (Figure S4, Supporting material) means that several pivotal interactions are shared to key residues in the NNIBP. This similarity is apparent when the hits (Compound 2, 5, 6, 11, 12, 15) and NNRTI are superimposed (Figure 6(A)). The "horseshoe-like" binding mode (Figure 1) showed hydrogen bond with residue Lys101/103, reported as an essential principle regarding NNRTI binding to HIV-1 RT (Das, Lewi, Hughes, & Arnold, 2005; Jorgensen et al., 2006; Kuroda et al., 2013; Nizami, Sydow, Wolber, & Honarparvar, 2016). All these characteristics suggested that the 23 hits may inhibit the activity of HIV-1 reverse transcriptase by similar mechanisms as known NNRTIs.

Table 2. The name, structural type, docking score, and references of 23 hits.

No.	Name	Structural type	Docking score	References
1	Pallidisetin A	Bibenzyl	−12.5	(Zheng et al., 1994; Ivanova et al., 2007)
2	Pallidisetin B	Bibenzyl	−12.2	
3	2-(4-methylpenta-1,3-dienyl) anthraquinone	Anthraquinone	−11.7	(Furumoto, Iwata, Hasan, & Fukui, 2003)
4	2-(4-methylpent-3-enyl) anthraquinone	Anthraquinone	−11.5	
5	Licoflavone C	Flavonoid	−11.2	(Pistelli, Bertoli, Giachi, & Manunta, 1998)
6	Kosamol S	Flavonoid	−11.0	(Zhang et al., 2007)
7	Glabranin	Flavonoid	−11.0	(Iuldashev, Batirov, Vdovin, & Abdullaev, 2000)
8	Glepidotin A	Flavonoid	−10.5	(Manfredi, Vallurupalli, Demidova, Kindscher, & Pannell, 2001)
9	Anhydronotoptol	Coumadin	−11.6	(Kozawa, Fukumoto, Matsuyama, & Baba, 1983)
10	Bergamottin	Coumadin	−11.2	(He et al., 1998)
11	Parabenzlactone	Lignan	−11.1	(Chen & Zhongcaoyao, 1986)
12	Hinokinin	Lignan	−10.9	(Kijjoa, Pinto, Tantisewie, & Herz, 1989; Cheng et al., 2005; Marcotullio, Pelosi, & Curini, 2014)
13	(-)-Stephalagine	Alkaloid	−11.6	(Dagne, Gunatilaka, Kingston, & Alemu, 1993)
14	Norstephalagine	Alkaloid	−11.3	(Cortes et al., 1990)
15	Morusyunnansin F	Flavonoid	−11.4	(Hu et al., 2012)
16	Typharin	Coumadin	−10.6	(Shode, Mahomed, & Rogers, 2002)
17	Diospongin B	Diarylheptanoid	−10.8	(Yin et al., 2004)
18	(3S,7S)-5,6-dehydro-4″-de-O-methylcentrolobine	Diarylheptanoid	−11.1	(Kadota, Tezuka, Prasain, Ali, & Banskota, 2003)
19	Mahanimbine	Alkaloid	−10.6	(Das, Chakraborty, & Bose, 1965)
20	Isolobelanine	Alkaloid	−10.7	(Chen, Chen, Zhang, Long, & Wang, 2014)
21	3-[2-(1,3-benzodioxol-5-yl)-7-methoxy-1-benzofuran-5-yl]propylbenzoate	Lignan	−10.0	(Ozturk, Akgul, & Anil, 2008)
22	Umbelliprenin	Coumadin	−10.1	(Abu-Mustafa, el-Bay, & Fayez, 1971)
23	5-(γ,γ-dimethylallyl)-oxyresveratrol	Polyphenol	−10.3	(Su et al., 2002)

3.4. External experimental consistency

Additionally, chemical scaffolds possessed by some hits, such as flavonoid (Compound 5, 6, 7, 8), coumadin (Compound 9, 10, 16, 22), anthraquinone (Compound 3, 4), and polyphenol (Compound 23) were structurally identical with anti-HIV or antiviral compounds recognized by the medical community (Ng, Huang, Fong, & Yeung, 1997; Zakaryan, Arabyan, Oo, & Zandi, 2017), such as Baicalein (Ono, Nakane, Fukushima, Chermann, & Barre-Sinoussi, 1989), Baicalin (Li et al., 1993; Kitamura et al., 1998), O-Demethylbuchenavianine (Beutler, Cardellina, McMahon, Boyd, & Cragg, 1992), Phenprocoumon (Kirkiacharian et al., 2002), Imperatorin (Zhou et al., 2000; Sancho et al., 2004), Resveratrol (Piao, Feng, Wang, Zhang, & Lin, 2010) and Emodin (Higuchi et al., 1991; Esposito, Corona, Zinzula, Kharlamova, & Tramontano, 2012) (Figure 6(B)). Benzofuran derivatives (Compound 21) also received more attention for their potential of anti-HIV-1 activity (El-Hawash & Wahab, 2006; Qin et al., 2006). Details of their measured anti-HIV activities are listed in Table 3. Additionally, the predicted IC50 value of 23 hits on HIV-RT are detailed in Table S7, Supporting material.

Notably, (+)-Hinokinin (Compound 12), a widely distributed lignan in several plants, was also reported for significant *in vitro* anti-HIV activity (IC50 values of 1.87 μg/mL) (Cheng, Lee, Tsai, & Chen, 2005). Moreover, both lignan derivative compound 11 and 12 shared similar binding mode with approved NNRTIs. These lignan derivatives (compound 11, 12) share identical chemical scaffolds as well. On the basis of the external experimental consistency, elaborated above, the proposed docking protocol in this study was possibly feasible and trustworthy.

3.5. Molecular dynamics simulations

The top 3 hits with highest docking score and similar binding poses (Figure 4) were selected from 23 screened compounds for further prediction. Molecular dynamics simulations were employed to investigate the binding stability of control and three hits using dynamic trajectories.

The RMSD of backbone atoms (including NNRTI motif), concerning the first frame of 30 ns production MD, is shown in Figure 7(A) and Figure S6(A,B), Supporting material.

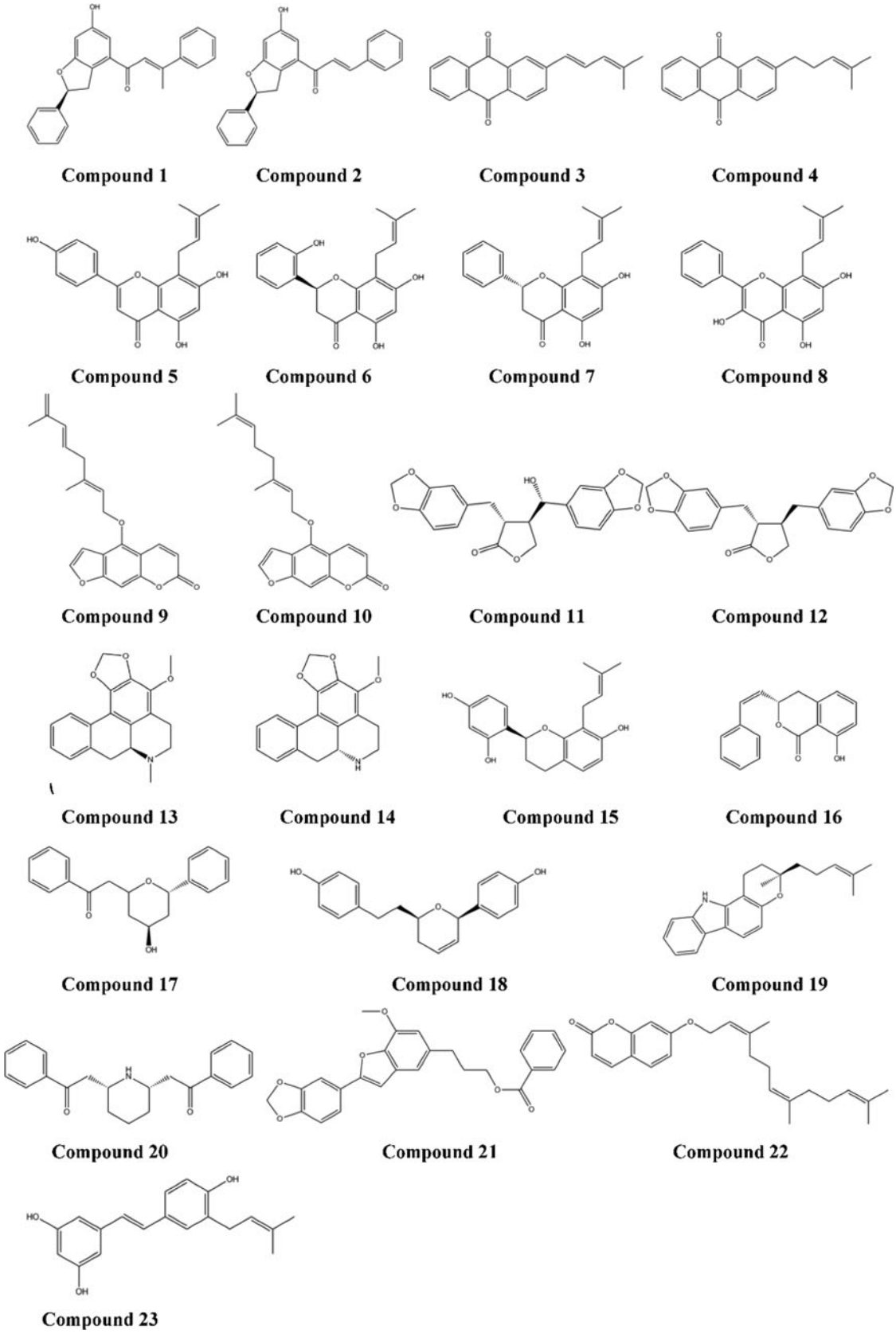

Figure 5. Two-dimensional structure of 23 natural molecules for potential NNRTIs identified by virtual screening.

Initially, sharp changes in backbone were observed followed by convergence. HIV-1 RT protein was documented as highly flexible in nature due to polymerization and RNase H activity (Rodgers et al., 1995; Das, Martinez, Bandwar, & Arnold, 2014). Whereas, average values of RMSD for RPV, C1, C2, and C3 in WT HIV-RT were recorded as 0.317 nm, 0.369 nm, 0.357 nm, and 0.468 nm, respectively. It had a similar behavior referred to the literature on HIV-1 RT with RMSD that

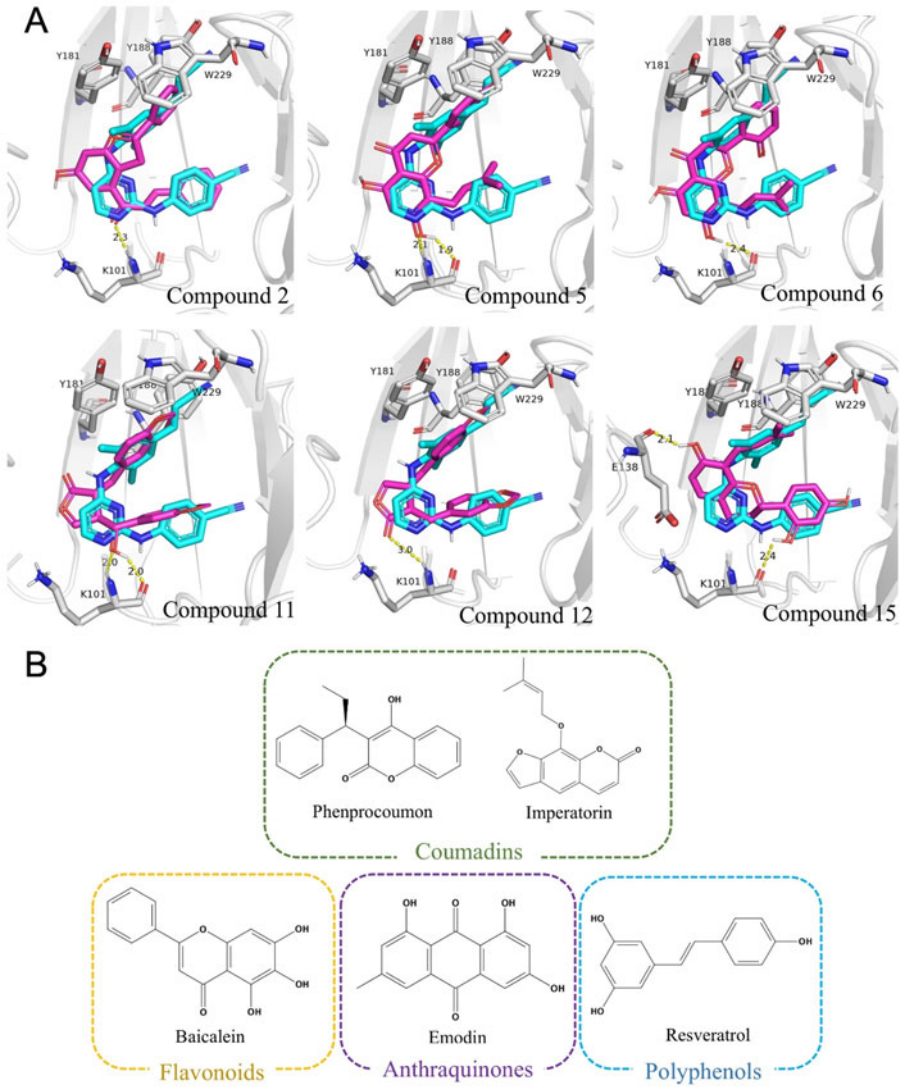

Figure 6. Binding mode and the structures of identified hits. (A) Representative horseshoes-like binding mode of some hits in NNIBP (PDB:4G1Q). The red stick represents the Rilpivirine, the blue stick represents the different hit compounds. (B) The structures of compounds with anti-HIV activity have been confirmed, including flavonoids, coumarins, anthraquinones, and polyphenols.

Table 3. Anti-HIV activity results of some natural compounds.

Compound name	Assay type	Anti-HIV activities
(+)-Hinokinin	*In vitro* anti-HIV	IC50 = 1.87 μg/mL
Baicalein	HIV-1 integrase	IC50 = 1.20 μmol/L
Baicalin	HIV-1 RT	IC50 = 31.17 μmol/L
	In vitro anti-HIV	EC50 = 0.5 μg/ml
O-Demethylbuchenavianine	*In vitro* anti-HIV	EC50 = 0.26 μmol/L
Phenprocoumon	HIV-1 protease	IC50 = 1 μmol/L
Imperatorin	*In vitro* anti-HIV	EC50 < 0.10 μg/mL
Resveratrol	*In vitro* anti-HIV	IC50 = 8.76 μmol/L
Emodin	*In vitro* anti-HIV	EC50 = 11.44 μmol/L
Concentricolide (Benzofuran derivative)	*In vitro* anti-HIV	EC50 = 0.31 μg/mL

validated the system's stability(Madrid, Jacobo-Molina, Ding, & Arnold, 1999; Temiz & Bahar, 2002). Also, a similar trend has been observed in the mutant HIV-RT protein systems (Figure S6(A,B), Supporting material). Concerning individual ligands, RMSDs of controls and hits suggested that all ligands bind to the receptor throughout the simulation. In addition to C3 (more than 0.1 nm), all ligand fluctuations were in a range of less than 0.05 nm. Moreover, RMSF results showed stability of NNIBP with ligands from residues 95 to 240 (Figure 7(B)), which was consistent with the earlier simulation study (Nizami et al., 2016). Further, the changes in complex compactness were also analyzed by calculating the Rg for the systems. The average values of Rg for RPV, C1, C2, and C3 were recorded as 3.41 nm, 3.50 nm, 3.46 nm, and 3.54 nm, respectively. These results indicated that the target protein folded correctly and able to keep a stable, compact structure (Figure 7(C)).

Generally, binding of the top 3 hits did not significantly alter the protein characteristics in comparison with controls (RPV and NVP) through C3 stability variation.

3.6. Binding free energy calculations to predict the binding affinity

The binding free energy estimates the binding affinity between ligand and RT. Average free energy of the solvation and other MM energy components were given in Table 4. Among the top three hits, C1 and C2 resulted in highest free binding energy in WT RT system. The calculated binding free

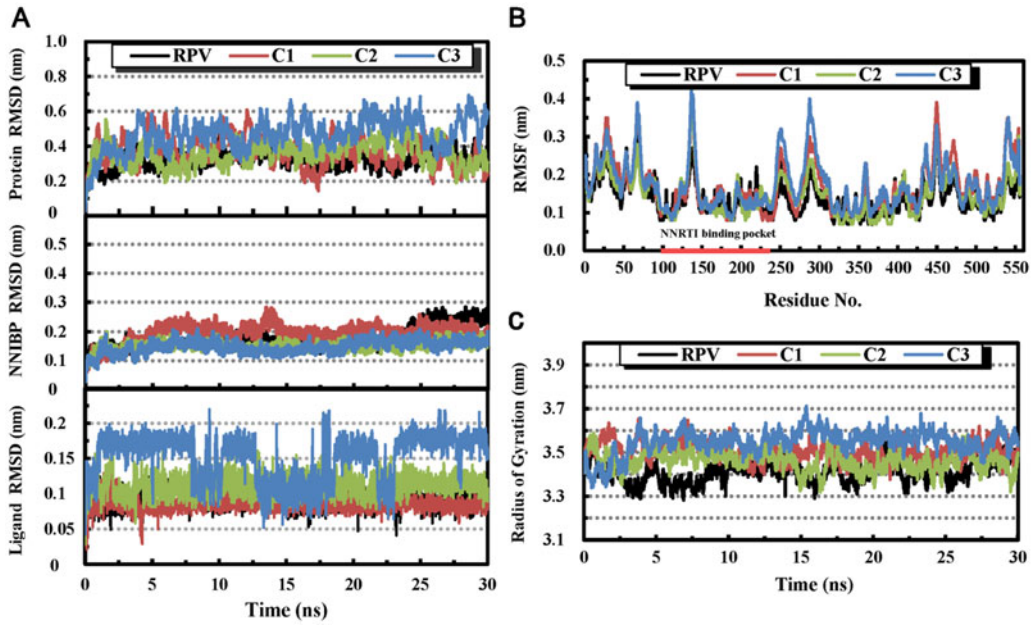

Figure 7. MD simulation results of Rilpivirine and top three candidates in complex with wild type HIV-RT protein during 30 ns simulation. (A) Root mean square deviation (RMSD) plot of backbone atoms (top), NNIBP (middle) and ligands (bottom). (B) Root mean square fluctuation (RMSF) of HIV-1 RT residues in the global motions of ligand-bound complexes. The region (from residues 95 to 240) of NNRTI binding pocket are indicated by a red underline. (C) The radius of gyrations (Rg) of proteins.

Table 4. Comparison of binding affinities of approved drugs with candidate hits.

Variants	Ligand	ΔG_{bind}	ΔE_{ele}	ΔE_{vdw}	ΔG_{SA}	ΔG_{polar}
WT	RPV	−29.33	−4.26	−49.78	−4.95	29.64
	C1	−31.71	−7.38	−44.75	−4.89	25.30
	C2	−31.78	−9.46	−42.36	−4.81	24.85
	C3	−26.08	−1.25	−31.32	−3.77	10.25
L100I K103N	RPV	−26.83	−2.99	−46.58	−4.95	27.67
	C1	−29.96	−5.01	−45.13	−5.03	25.01
	C2	−30.17	−3.98	−41.56	−4.25	19.59
K101E	NVP	−25.89	−4.09	−39.29	−3.76	21.24
	C1	−28.07	−5.71	−44.39	−4.57	26.54
	C2	−28.81	−6.34	−45.51	−4.10	27.46

The binding free energy (ΔG_{bind} in kcal mol^{-1}) and different energy components, such as electrostatic energy (ΔE_{ele}), van der Waals (ΔE_{vdW}), and solvation energy (ΔG_{SA} and ΔG_{polar}) for the wide-type and mutant complex.

energy (ΔG_{bind}) of 29.33 kcal/mol for RPV compared to WT RT protein was 31.71 and 31.78 kcal/mol for C1 and C2, respectively. Also, ΔG_{bind} of C3 showed lower binding energy of 26.08 kcal/mol. The L100I/K103N mutant had lower ΔG_{bind} (−26.84 kcal/mol), inferring significant reduction in interactions of RPV (third-generation NNRTI) with residues at the NNIBP. A similar trend was also observed for ΔG_{bind} of NVP (first generation NNRTI) complexed with K101E HIV-RT, suggesting that it can drastically lose their binding potency against NNRTI-resistance mutations. This observation was consistent with the previous reports that confirmed the feasibility of our assessment method (Johnson et al., 2008). Moreover, it is noteworthy that both C1 and C2 have higher ΔG_{bind} in L100I/K103N double mutant and K101E single mutant complexes as compared to that of two controls, and binding ability of 2 hits was equivalent. Additionally, electrostatic interactions played a critical role in binding energy even in the hydrophobic binding pocket and were partially responsible for the inhibitor binding affinity towards multiple RT variants(Kroeger Smith et al., 1995; Minkara, Davis, & Radhakrishnan, 2012). It was also observed that ΔE_{ele} of C1 and C2 was higher against that of controls, which acted as favorable and contributing factor to the high binding affinity and stability.

3.7. Dynamic binding behavior of top 2 hits in NNIBP during MD simulation

Top 2 hits (Pallidisetin A and Pallidisetin B), that showed better performance through binding free energy, were selected to analyze their binding modes with HIV-RT. It was noted that the two hits bind in the hydrophobic pocket form a stable "horseshoe-shape" combination in both WT and MT during MD trajectory (Figure 8 and Figure S7, Supporting material). The H-bond distance profiles (Figure 9) and frequency between the RT (WT and MT) and ligands at NNIBP are summarized in Table S10, Supporting material. It observed that the control RPV could form a stable hydrogen bond interaction between RPV and Lys101 from 1.7 to 30 ns (Figure 9(A)). In WT, both Pallidisetin A and Pallidisetin B appeared to form a strong H-bonds interaction with the oxygen atom of Lys101, with the high bond frequency of 83.4% and 85.5%, respectively. Also, a stable interaction between Pallidisetin B and Lys103 was recorded. Interacting with critical residues (K101/K103) on NNIBP is a conventional mechanism for "U-shape" or "horseshoe" NNRTIs mediated inhibition of RT which was reported in crystallographic studies and computational studies (Zhan et al., 2013).

Commonly, mutations at the residues 101 and 103 will develop significant drug-resistance to most NNRTIs (Byrnes et al., 1993; Rubsamen-Waigmann et al., 1999). NNRTI-resistance mutations affect NNRTI binding directly or indirectly by altering hydrophobic and electrostatic interaction between the inhibitors and NNIBP (Das et al., 2005). Interestingly,

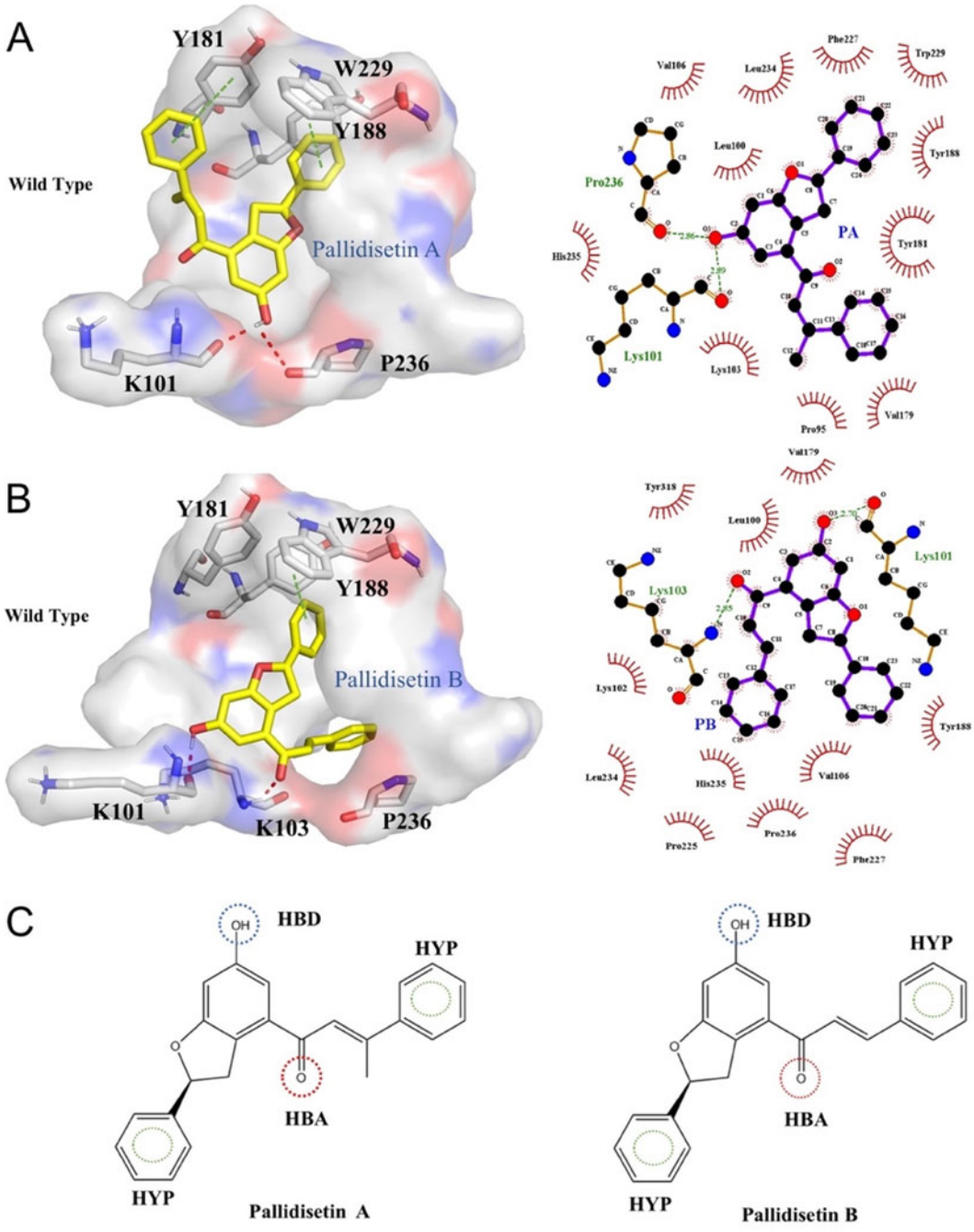

Figure 8. The binding mode and pharmacophore model of top 2 hits. (A) The representative binding mode of Pallidisetin A in NNIBP of WT RT. (B)The binding mode of Pallidisetin B in NNIBP of WT RT. Hydrogen bond interactions are shown by red dotted lines, while π-π stacking interaction are shown as green dotted lines (left). Hydrogen bonds in 2D ligand-protein interaction diagrams are shown as green dotted lines, while the spoked arcs represent protein residues making nonbonded contacts with the ligand (right). The snapshots were obtained from MD trajecties (C) The key features of top 2 hits for designing NNRTI targeting HIV-1 RT. Hydrogen bond donor (HBD), hydrogen bond acceptor (HBA) and hydrophobic regions (HPY) were indicated by blue, red and green dashed circle, respectively.

compared to the corresponding WT structure, two hits bind to the mutant in a conservative mode. As shown in Figure 9(C) and Figure S7(A), Supporting material, both two hits accommodate in the K101E mutation by forming new interactions to the Glu101 or Pro236 side chain. These alternatives H-bond with K101 or P236/H235 in the binding mode were also observed even in L100I/K103N double variant (Figure 9(D) and Figure S7(B), Supporting material). However, H-bond distance fluctuated overtime periodically and this shift may be attributed to the change of conformation in 101 or 103 position residues. As illustrated in Figure 9(D) (top), Pallidisetin A also formed transient interactions to Asn103 during last 10 ns. The binding behavior which compensated the loss of H-bond interaction caused by mutations and the same mechanism with the efficacy of inhibitors against MT RT has been reported in earlier studies (Hsiou et al., 1998; Hogberg et al., 2000). Such positional adaptability appeared to be critical for retaining the potency and improving resilience to drug-resistant variants.

Pallidisetin A and Pallidisetin B are derived from bryophyte (*Polytrichum pallidisetum*), with the same scaffold. Phenolic hydroxyl group and the carbonyl group of compounds favored

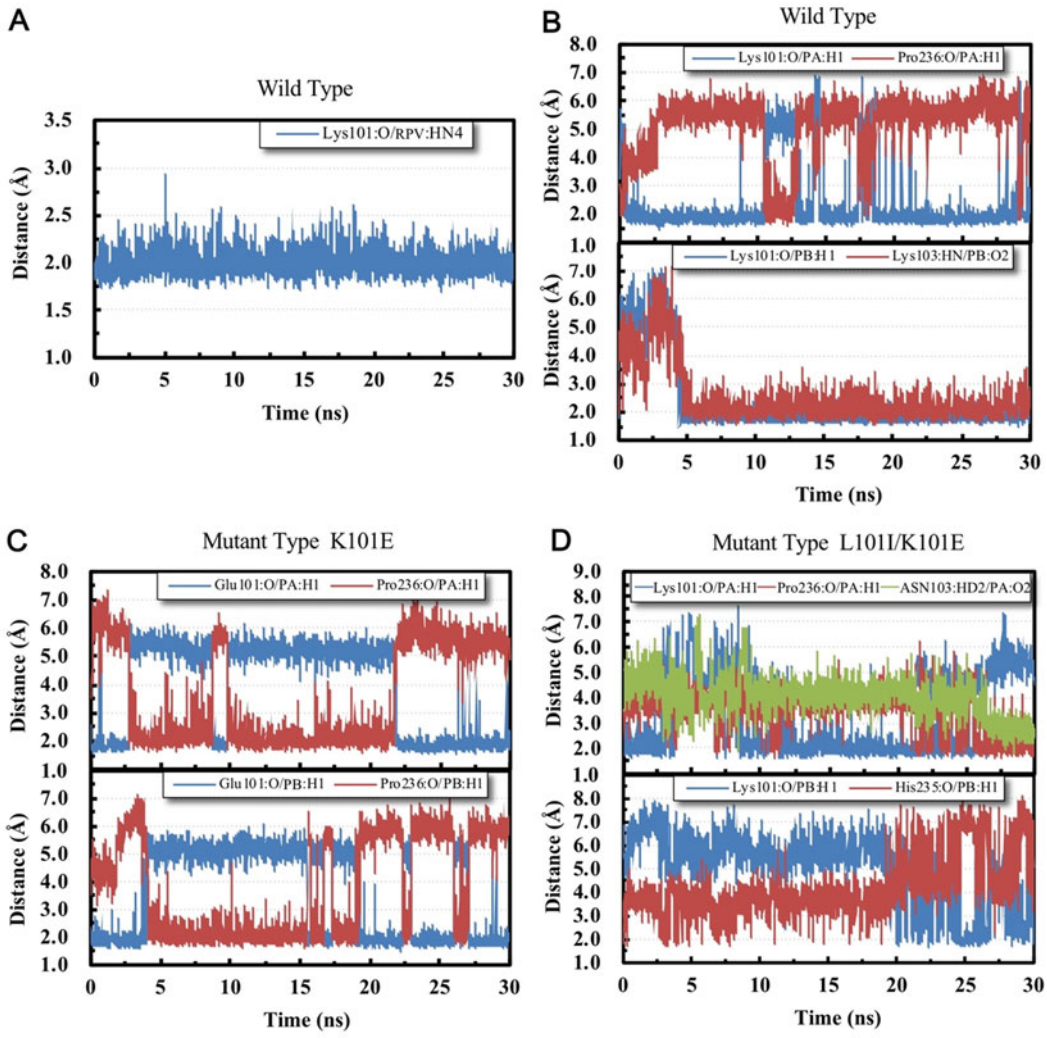

Figure 9. The comparison of hydrogen bond distance profiles of Rilpivirine (RPV), Pallidisetin A (top) and Pallidisetin B (bottom) bound with HIV-RT protein during MD simulation. (A) Rilpivirine in WT-RT, (B) Pallidisetin A and Pallidisetin B in WT- RT, (C) Pallidisetin A and Pallidisetin B in K101E mutant- RT, (D) Pallidisetin A and Pallidisetin B in L100I/K103N mutant-RT.

to act as H-bond donor to K101/E101 or H-bond acceptors to E101/K103. Two aromatic ring groups have hydrophobic or π-π stacking effect (Y188, Y181, and W229) with residues (such as Y188, Y181, W229, F227, L100, L234, and Y318) located at the interior part of NNIBP, which can potentially enhance the binding strength to HIV-RT protein. These key chemical features (Figure 8(C)) conformed with '3-point pharmacophore model' which have been demonstrated by HIV-RT complexes information and computational programs (Daeyaert et al., 2004; Daszykowski et al., 2004).

4. Conclusion

In this study, 23 natural molecules with favorable properties were identified as potential NNRTIs from TCM databases. One hit shows obvious HIV-1 inhibitory effect, and 12 hits have special scaffolds (such as flavonoid, coumadin, anthraquinone, and polyphenol) consistent with external experimental results, showing anti-HIV potentiality. Many compounds among the hits shared a similar binding mode as observed in approved NNRTIs complexed with RT structures. Finally, supported by the high binding affinity and binding stability through molecular simulation analysis, we can conclude that the herbal derived low toxic compounds, Pallidisetin A and Pallidisetin B, may have broad antimutant spectrum. However, further *in vitro* and *in vivo* validations are required to fully substantiate and confirm the inhibitory efficacy of Pallidisetin A and Pallidisetin B. It is thus can be safely drawn that these identified hits will serve as a promising starting point for broad spectrum anti-HIV agents. The overall strategy proposed in this work is a feasible and trustworthy way to propose potential scaffolds with broad anti-resistance spectrum for HIV RT, and TCM is a valuable fountain for anti-HIV drug discovery.

Disclosure statement

The authors declare that there are no competing interests.

Funding

This work was supported by the funding from National Key Research Program (Contract No.2016YFA0501703), National Natural Science Foundation of China (Grant No. 31601074, 61872094, 61832019), and

Shanghai Jiao Tong University School of Medicine (Contract No. YG2017ZD14).

References

Abu-Mustafa, E. A., el-Bay, F. K., & Fayez, M. B. (1971). Natural coumarins. XII. Umbelliprenin, a constituent of ammi majus L. fruits. *Journal of Pharmaceutical Sciences*, *60*(5), 788–789. doi:10.1002/jps.2600600528

Acuna, U. M., Jancovski, N., & Kennelly, E. J. (2009). Polyisoprenylated benzophenones from Clusiaceae: Potential drugs and lead compounds. *Current Topics in Medicinal Chemistry*, *9*(16), 1560–1580.

Andersson, D. I., & Levin, B. R. (1999). The biological cost of antibiotic resistance. *Current Opinion in Microbiology*, *2*(5), 489–493.

Battini, L., & Bollini, M. (2019). Challenges and approaches in the discovery of human immunodeficiency virus type-1 non-nucleoside reverse transcriptase inhibitors. *Medicinal Research Reviews*, *39*(4), 1235–1273. doi:10.1002/med.21544

Bauman, J. D., Das, K., Ho, W. C., Baweja, M., Himmel, D. M., Clark, A. D., … Arnold, E. (2008). Crystal engineering of HIV-1 reverse transcriptase for structure-based drug design. *Nucleic Acids Research*, *36*(15), 5083–5092. doi:10.1093/nar/gkn464

Best, R. B., Zhu, X., Shim, J., Lopes, P. E., Mittal, J., Feig, M., & Mackerell, A. D., Jr. (2012). Optimization of the additive CHARMM all-atom protein force field targeting improved sampling of the backbone phi, psi and side-chain chi(1) and chi(2) dihedral angles. *Journal of Chemical Theory and Computation*, *8*(9), 3257–3273. doi:10.1021/ct300400x

Beutler, J. A., Cardellina, J. H., II, McMahon, J. B., Boyd, M. R., & Cragg, G. M. (1992). Anti-HIV and cytotoxic alkaloids from Buchenavia capitata. *Journal of Natural Products*, *55*(2), 207–213.

Broder, S. (2010). The development of antiretroviral therapy and its impact on the HIV-1/AIDS pandemic. *Antiviral Research*, *85*(1), 1–18. doi:10.1016/j.antiviral.2009.10.002

Byrnes, V. W., Sardana, V. V., Schleif, W. A., Condra, J. H., Waterbury, J. A., Wolfgang, J. A., … Wolanski, B. S. (1993). Comprehensive mutant enzyme and viral variant assessment of human immunodeficiency virus type 1 reverse transcriptase resistance to nonnucleoside inhibitors. *Antimicrobial Agents and Chemotherapy*, *37*(8), 1576–1579. doi:10.1128/AAC.37.8.1576

Chen, C. Y. (2011). TCM Database@Taiwan: The world's largest traditional Chinese medicine database for drug screening in silico. *PLoS One*, *6*(1), e15939. doi:10.1371/journal.pone.0015939

Chen, M. W., Chen, W. R., Zhang, J. M., Long, X. Y., & Wang, Y. T. (2014). Lobelia chinensis: Chemical constituents and anticancer activity perspective. *Chinese Journal of Natural Medicines*, *12*(2), 103–107. doi:10.1016/S1875-5364(14)60016-9

Chen, R. T., & Zhongcaoyao, D. S. F. (1986). Chemical constituents of *Torreya jackii*. HI. Structure of torreyinol. *Chinese Traditional and Herbal Drugs*, *17*, 566.

Cheng, M. J., Lee, K. H., Tsai, I. L., & Chen, I. S. (2005). Two new sesquiterpenoids and anti-HIV principles from the root bark of *Zanthoxylum ailanthoides*. *Bioorganic & Medicinal Chemistry*, *13*(21), 5915–5920. doi:10.1016/j.bmc.2005.07.050

Clutter, D. S., Jordan, M. R., Bertagnolio, S., & Shafer, R. W. (2016). HIV-1 drug resistance and resistance testing. *Infection Genetics and Evolution*, *46*, 292–307. doi:10.1016/j.meegid.2016.08.031

Cortes, D., Torrero, M. Y., Pilar D'Ocon, M., Luz Candenas, M., Cave, A., & Hadi, A. H. (1990). [Norstephalagine and atherospermidine: Two smooth muscle relaxant aporphines from Artabotrys maingayi]. *Journal of Natural Products*, *53*(2), 503–508.

Creagh, T., Ruckle, J. L., Tolbert, D. T., Giltner, J., Eiznhamer, D. A., Dutta, B., … Xu, Z.-Q. (2001). Safety and pharmacokinetics of single doses of (+)-calanolide a, a novel, naturally occurring nonnucleoside reverse transcriptase inhibitor, in healthy, human immunodeficiency virus-negative human subjects. *Antimicrobial Agents and Chemotherapy*, *45*(5), 1379–1386. doi:10.1128/AAC.45.5.1379-1386.2001

Daeyaert, F., de Jonge, M., Heeres, J., Koymans, L., Lewi, P., Vinkers, M. H., & Janssen, P. A. (2004). A pharmacophore docking algorithm and its application to the cross-docking of 18 HIV-NNRTI's in their binding pockets. *Proteins: Structure, Function, and Bioinformatics*, *54*(3), 526–533. doi:10.1002/prot.10599

Dagne, E., Gunatilaka, A. A., Kingston, D. G., & Alemu, M. (1993). 4′-O-methylstephavanine from Stephania abyssinica. *Journal of Natural Products*, *56*(11), 2022–2025.

Das, K., Lewi, P. J., Hughes, S. H., & Arnold, E. (2005). Crystallography and the design of anti-AIDS drugs: Conformational flexibility and positional adaptability are important in the design of non-nucleoside HIV-1 reverse transcriptase inhibitors. *Progress in Biophysics and Molecular Biology*, *88*(2), 209–231. doi:10.1016/j.pbiomolbio.2004.07.001

Das, K., Martinez, S. E., Bandwar, R. P., & Arnold, E. (2014). Structures of HIV-1 RT-RNA/DNA ternary complexes with dATP and nevirapine reveal conformational flexibility of RNA/DNA: Insights into requirements for RNase H cleavage. *Nucleic Acids Research*, *42*(12), 8125–8137. doi:10.1093/nar/gku487

Das, K. C., Chakraborty, D. P., & Bose, P. K. (1965). Antifungal activity of some constituents of Murraya koenigii Spreng. *Experientia*, *21*(6), 340. doi:10.1007/BF02144703

Daszykowski, M., Walczak, B., Xu, Q.-S., Daeyaert, F., de Jonge, M. R., Heeres, J., … Massart, D. L. (2004). Classification and regression trees-studies of HIV reverse transcriptase inhibitors. *Journal of Chemical Information and Computer Sciences*, *44*(2), 716–726. doi:10.1021/ci034170h

de Bethune, M. P. (2010). Non-nucleoside reverse transcriptase inhibitors (NNRTIs), their discovery, development, and use in the treatment of HIV-1 infection: A review of the last 20 years (1989–2009. *Antiviral Research*, *85*(1), 75–90. doi:10.1016/j.antiviral.2009.09.008

De Clercq, E. (2002). Strategies in the design of antiviral drugs. *Nature Reviews Drug Discovery*, *1*(1), 13–25. doi:10.1038/nrd703

Delaugerre, C., Rohban, R., Simon, A., Mouroux, M., Tricot, C., Agher, R., … Calvez, V. (2001). Resistance profile and cross-resistance of HIV-1 among patients failing a non-nucleoside reverse transcriptase inhibitor-containing regimen. *Journal of Medical Virology*, *65*(3), 445–448. doi:10.1002/jmv.2055

El-Hawash, S. A. M., & Wahab, A. E. A. (2006). Synthesis and in vitro-anticancer and antimicrobial evaluation of some novel quinoxalines derived from 3-phenylquinoxaline-2(1H)-thione. *Archiv Der Pharmazie*, *339*(8), 437–447. doi:10.1002/ardp.200600012

Esposito, F., Corona, A., Zinzula, L., Kharlamova, T., & Tramontano, E. (2012). New Anthraquinone derivatives as inhibitors of the HIV-1 reverse transcriptase-associated ribonuclease H function. *Chemotherapy*, *58*(4), 299–307. doi:10.1159/000343101

Furumoto, T., Iwata, M., Hasan, A. F. M. F., & Fukui, H. (2003). Anthrasesamones from roots of *Sesamum indicum*. *Phytochemistry*, *64*(4), 863–866. doi:10.1016/j.phytochem.2003.09.004

Gottlieb, M. S., Schroff, R., Schanker, H. M., Weisman, J. D., Fan, P. T., Wolf, R. A., & Saxon, A. (1981). Pneumocystis carinii pneumonia and mucosal candidiasis in previously healthy homosexual men: Evidence of a new acquired cellular immunodeficiency. *New England Journal of Medicine*, *305*(24), 1425–1431. doi:10.1056/NEJM198112103052401

He, K., Iyer, K. R., Hayes, R. N., Sinz, M. W., Woolf, T. F., & Hollenberg, P. F. (1998). Inactivation of cytochrome P450 3A4 by bergamottin, a component of grapefruit juice. *Chemical Research in Toxicology*, *11*(4), 252–259. doi:10.1021/tx970192k

Hess, B., Kutzner, C., Van Der Spoel, D., & Lindahl, E. (2008). GROMACS 4: Algorithms for highly efficient, load-balanced, and scalable molecular simulation. *Journal of Chemical Theory and Computation*, *4*(3), 435–447. doi:10.1021/ct700301q

Higuchi, H., Mori, K., Kato, A., Ohkuma, T., Endo, T., Kaji, H., & Kaji, A. (1991). Antiretroviral activities of anthraquinones and their inhibitory effects on reverse transcriptase. *Antiviral Research*, *15*(3), 205–216. doi:10.1016/0166-3542(91)90067-2

Hogberg, M., Sahlberg, C., Engelhardt, P., Noreen, R., Kangasmetsa, J., Johansson, N. G., … Backbro, K. (2000). Urea-PETT compounds as a new class of HIV-1 reverse transcriptase inhibitors. 3. Synthesis and further structure-activity relationship studies of PETT analogues. (vol. 42, pg 4145, 1999). *Journal of Medicinal Chemistry*, *43*(2), 304–304. doi:10.1021/jm990572y

Hsiou, Y., Das, K., Ding, J., Clark, A. D., Kleim, J.-P., Rösner, M., … Arnold, E. (1998). Structures of Tyr188Leu mutant and wild-type HIV-1 reverse transcriptase complexed with the non-nucleoside inhibitor HBY 097: Inhibitor flexibility is a useful design feature for reducing drug resistance. *Journal of Molecular Biology*, *284*(2), 313–323. doi:10.1006/jmbi.1998.2171

Hsiou, Y., Ding, J., Das, K., Clark, A. D., Jr., Hughes, S. H., & Arnold, E. (1996). Structure of unliganded HIV-1 reverse transcriptase at 2.7 A resolution: Implications of conformational changes for polymerization and inhibition mechanisms. *Structure*, *4*(7), 853–860. doi:10.1016/S0969-2126(96)00091-3

Hu, X., Wu, J. W., Wang, M., Yu, M. H., Zhao, Q. S., Wang, H. Y., & Hou, A. J. (2012). 2-Arylbenzofuran, flavonoid, and tyrosinase inhibitory constituents of Morus yunnanensis. *Journal of Natural Products*, *75*(1), 82–87. doi:10.1021/np2007318

Humphrey, W., Dalke, A., & Schulten, K. (1996). VMD: Visual molecular dynamics. *Journal of Molecular Graphics*, *14*(1), 27–38.

Iuldashev, M. P., Batirov, E., Vdovin, A. D., & Abdullaev, N. D. (2000). [Glabrizoflavone-a novel isoflavone from Glycyrrhiza glabra L]. *Bioorganicheskaia Khimiia*, *26*(11), 873–876. [

Ivanova, V., Kolarova, M., Aleksieva, K., Dornberger, K.-J., Haertl, A., Moellmann, U., … Chipev, N. (2007). Sanionins: Anti-inflammatory and antibacterial agents with weak cytotoxicity from the Antarctic moss *Sanionia georgico-uncinata*. *Preparative Biochemistry and Biotechnology*, *37*(4), 343–352. doi:10.1080/10826060701593241

Janssen, P. A. J., Lewi, P. J., Arnold, E., Daeyaert, F., de Jonge, M., Heeres, J., … Stoffels, P. (2005). In search of a novel anti-HIV drug: Multidisciplinary coordination in the discovery of 4-[[4-[[4-[(1E)-2-cyanoethenyl]-2,6-dimethylphenyl]amino]-2-pyrimidinyl]amino]benzonitrile (R278474, rilpivirine). *Journal of Medicinal Chemistry*, *48*(6), 1901–1909. doi:10.1021/jm040840e

Johnson, J. A., Li, J.-F., Wei, X., Lipscomb, J., Irlbeck, D., Craig, C., … Heneine, W. (2008). Minority HIV-1 drug resistance mutations are present in antiretroviral treatment-naive populations and associate with reduced treatment efficacy. *Plos Medicine*, *5*(7), e158–1122. doi:ARTN e158 doi:10.1371/journal.pmed.0050158

Jorgensen, W. L., Ruiz-Caro, J., Tirado-Rives, J., Basavapathruni, A., Anderson, K. S., & Hamilton, A. D. (2006). Computer-aided design of non-nucleoside inhibitors of HIV-1 reverse transcriptase. *Bioorganic & Medicinal Chemistry Letters*, *16*(3), 663–667. doi:10.1016/j.bmcl.2005.10.038

Kadota, S., Tezuka, Y., Prasain, J. K., Ali, M. S., & Banskota, A. H. (2003). Novel diarylheptanoids of Alpinia blepharocalyx. *Current Topics in Medicinal Chemistry*, *3*(2), 203–225.

Kijjoa, A., Pinto, M. M., Tantisewie, B., & Herz, W. (1989). A new linalool derivative and other constituents from Piper ribesoides. *Planta Medica*, *55*(2), 193–194. doi:10.1055/s-2006-961923

Kirkiacharian, S., Thuy, D. T., Sicsic, S., Bakhchinian, R., Kurkjian, R., & Tonnaire, T. (2002). Structure-activity relationships of some 3-substituted-4-hydroxycoumarins as HIV-1 protease inhibitors. *Farmaco*, *57*(9), 703–708. doi:Pii S0014-827x(02)01264-8 doi:10.1016/S0014-827X(02)01264-8

Kitamura, K., Honda, M., Yoshizaki, H., Yamamoto, S., Nakane, H., Fukushima, M., … Tokunaga, T. (1998). Baicalin, an inhibitor of HIV-1 production in vitro. *Antiviral Research*, *37*(2), 131–140.

Koch, M. A., Schuffenhauer, A., Scheck, M., Wetzel, S., Casaulta, M., Odermatt, A., … Waldmann, H. (2005). Charting biologically relevant chemical space: A structural classification of natural products (SCONP). *Proceedings of the National Academy of Sciences of the United States of America*, *102*(48), 17272–17277. doi:10.1073/pnas.0503647102

Kozawa, M., Fukumoto, M., Matsuyama, Y., & Baba, K. (1983). Chemical studies on the constituents of the Chinese crude drug "Quiang Huo". *Chemical & Pharmaceutical Bulletin*, *31*(8), 2712–2717. doi:10.1248/cpb.31.2712

Kroeger Smith, M. B., Hughes, S. H., Boyer, P. L., Michejda, C. J., Rouzer, C. A., Taneyhill, L. A., … Zhang, W. (1995). Molecular modeling studies of HIV-1 reverse transcriptase nonnucleoside inhibitors: Total energy of complexation as a predictor of drug placement and activity. *Protein Science*, *4*(10), 2203–2222. doi:10.1002/pro.5560041026

Kumari, R., Kumar, R., Open Source Drug Discovery Consortium, & Lynn, A. (2014). g_mmpbsa–a GROMACS tool for high-throughput MM-PBSA calculations. *Journal of Chemical Information and Modeling*, *54*(7), 1951–1962. doi:10.1021/ci500020m

Kurapati, K. R. V., Atluri, V. S., Samikkannu, T., Garcia, G., & Nair, M. P. N. (2016). Natural products as anti-HIV agents and role in HIV-Associated Neurocognitive Disorders (HAND): A brief overview. *Frontiers in Microbiology*, *6*(212). doi:ARTN 1444 10.3389/fmicb.2015.01444

Kuroda, D. G., Bauman, J. D., Challa, J. R., Patel, D., Troxler, T., Das, K., … Hochstrasser, R. M. (2013). Snapshot of the equilibrium dynamics of a drug bound to HIV-1 reverse transcriptase. *Nature Chemistry*, *5*(3), 174–181. doi:10.1038/nchem.1559

Laskowski, R. A., & Swindells, M. B. (2011). LigPlot+: Multiple ligand-protein interaction diagrams for drug discovery. *Journal of Chemical Information and Modeling*, *51*(10), 2778–2786. doi:10.1021/ci200227u

Li, B. Q., Fu, T., Yan, Y. D., Baylor, N. W., Ruscetti, F. W., & Kung, H. F. (1993). Inhibition of HIV infection by baicalin–a flavonoid compound purified from Chinese herbal medicine. *Cellular & Molecular Biology Research*, *39*(2), 119–124.

Li, S., Hattori, T., & Kodama, E. N. (2011). Epigallocatechin gallate inhibits the HIV reverse transcription step. *Antiviral Chemistry and Chemotherapy*, *21*(6), 239–243. doi:10.3851/IMP1774

Li, X., Zhang, L., Tian, Y., Song, Y., Zhan, P., & Liu, X. (2014). Novel HIV-1 non-nucleoside reverse transcriptase inhibitors: A patent review (2011–2014). *Expert Opinion on Therapeutic Patents*, *24*(11), 1199–1227. doi:10.1517/13543776.2014.964685

Lu, X., Liu, L., Zhang, X., Lau, T. C. K., Tsui, S. K. W., Kang, Y., … Chen, Z. (2012). F18, a novel small-molecule nonnucleoside reverse transcriptase inhibitor, inhibits HIV-1 replication using distinct binding motifs as demonstrated by resistance selection and docking analysis. *Antimicrobial Agents and Chemotherapy*, *56*(1), 341–351. doi:10.1128/AAC.05537-11

Madrid, M., Jacobo-Molina, A., Ding, J., & Arnold, E. (1999). Major subdomain rearrangement in HIV-1 reverse transcriptase simulated by molecular dynamics. *Proteins: Structure, Function, and Genetics*, *35*(3), 332–337. doi:10.1002/(SICI)1097-0134(19990515)35:3<332::AID-PROT7>3.0.CO;2-R

Manfredi, K. P., Vallurupalli, V., Demidova, M., Kindscher, K., & Pannell, L. K. (2001). Isolation of an anti-HIV diprenylated bibenzyl from Glycyrrhiza lepidota. *Phytochemistry*, *58*(1), 153–157. doi:10.1016/S0031-9422(01)00177-7

Marcotullio, M. C., Pelosi, A., & Curini, M. (2014). Hinokinin, an emerging bioactive lignan. *Molecules*, *19*(9), 14862–14878. doi:10.3390/molecules190914862

Menendez-Arias, L. (2013). Molecular basis of human immunodeficiency virus type 1 drug resistance: Overview and recent developments. *Antiviral Research*, *98*(1), 93–120. doi:10.1016/j.antiviral.2013.01.007

Michaud-Agrawal, N., Denning, E. J., Woolf, T. B., & Beckstein, O. (2011). Software news and updates MDAnalysis: A toolkit for the analysis of molecular dynamics simulations. *Journal of Computational Chemistry*, *32*(10), 2319–2327. doi:10.1002/jcc.21787

Minkara, M. S., Davis, P. H., & Radhakrishnan, M. L. (2012). Multiple drugs and multiple targets: An analysis of the electrostatic determinants of binding between non-nucleoside HIV-1 reverse transcriptase inhibitors and variants of HIV-1 RT. *Proteins: Structure, Function, and Bioinformatics*, *80*(2), 573–590. doi:10.1002/prot.23221

Mysinger, M. M., Carchia, M., Irwin, J. J., & Shoichet, B. K. (2012). Directory of useful decoys, enhanced (DUD-E): Better ligands and decoys for better benchmarking. *Journal of Medicinal Chemistry*, *55*(14), 6582–6594. doi:10.1021/jm300687e

Namasivayam, V., Vanangamudi, M., Kramer, V. G., Kurup, S., Zhan, P., Liu, X., … Byrareddy, S. N. (2019). The journey of HIV-1 non-nucleoside reverse transcriptase inhibitors (NNRTIs) from lab to clinic. *Journal of Medicinal Chemistry*, *62*(10), 4851–4883. doi:10.1021/acs.jmedchem.8b00843

Ng, T. B., Huang, B., Fong, W. P., & Yeung, H. W. (1997). Anti-human immunodeficiency virus (anti-HIV) natural products with special emphasis on HIV reverse transcriptase inhibitors. *Life Sciences*, *61*(10), 933–949. doi:10.1016/S0024-3205(97)00245-2

Nizami, B., Sydow, D., Wolber, G., & Honarparvar, B. (2016). Molecular insight on the binding of NNRTI to K103N mutated HIV-1 RT: Molecular dynamics

simulations and dynamic pharmacophore analysis. *Molecular Biosystems*, *12*(11), 3385–3395. doi:10.1039/C6MB00428H

Ono, K., Nakane, H., Fukushima, M., Chermann, J. C., & Barre-Sinoussi, F. (1989). Inhibition of reverse transcriptase activity by a flavonoid compound, 5,6,7-trihydroxyflavone. *Biochemical and Biophysical Research Communications*, *160*(3), 982–987. doi:10.1016/S0006-291X(89)80097-X

Ozturk, S. E., Akgul, Y., & Anil, H. (2008). Synthesis and antibacterial activity of egonol derivatives. *Bioorganic & Medicinal Chemistry*, *16*(8), 4431–4437. doi:10.1016/j.bmc.2008.02.057

Palumbi, S. R. (2001). Humans as the world's greatest evolutionary force. *Science*, *293*(5536), 1786–1790. doi:10.1126/science.293.5536.1786

Piao, Z. S., Feng, Y. B., Wang, L., Zhang, X. Q., & Lin, M. (2010). Synthesis and HIV-1 inhibitory activity of natural products isolated from Gnetum parvifolium and their analogues. *Yao Xue Xue Bao*, *45*(12), 1509–1515.

Pistelli, L., Bertoli, A., Giachi, I. I., & Manunta, A. (1998). Flavonoids from genista ephedroides. *Journal of Natural Products*, *61*(11), 1404–1406. doi:10.1021/np980112s

Preston, B. D., Poiesz, B. J., & Loeb, L. A. (1988). Fidelity of HIV-1 reverse transcriptase. *Science (New York, N.Y.)*, *242*(4882), 1168–1171. doi:10.1126/science.2460924

Qin, X.-D., Dong, Z.-J., Liu, J.-K., Yang, L.-M., Wang, R.-R., Zheng, Y.-T., … Zheng, Q.-T. (2006). Concentricolide, an anti-HIV agent from the ascomycete *Daldinia concentrica*. *Helvetica Chimica Acta*, *89*(1), 127–133.

Qureshi, A., Rajput, A., Kaur, G., & Kumar, M. (2018). HIVprotI: An integrated web based platform for prediction and design of HIV proteins inhibitors. *Journal of Cheminformatics*, *10*(1), 12. doi:10.1186/s13321-018-0266-y

Ragno, R., Mai, A., Sbardella, G., Artico, M., Massa, S., Musiu, C., … La Colla, P. (2004). Computer-aided design, synthesis, and anti-HIV-1 activity in vitro of 2-alkylamino-6-[1-(2,6-difluorophenyl)alkyl]-3,4-dihydro-5-alkylpyrimidin-4(3H)-o nes as novel potent non-nucleoside reverse transcriptase inhibitors, also active against the Y181C variant. *Journal of Medicinal Chemistry*, *47*(4), 928–934. doi:10.1021/jm0309856

Roberts, J. D., Bebenek, K., & Kunkel, T. A. (1988). The accuracy of reverse transcriptase from HIV-1. *Science (New York, N.Y.)*, *242*(4882), 1171–1173. doi:10.1126/science.2460925

Rodgers, D. W., Gamblin, S. J., Harris, B. A., Ray, S., Culp, J. S., Hellmig, B., … Harrison, S. C. (1995). The structure of unliganded reverse transcriptase from the human immunodeficiency virus type 1. *Proceedings of the National Academy of Sciences of the United States of America*, *92*(4), 1222–1226. doi:10.1073/pnas.92.4.1222

Rubsamen-Waigmann, H., Huguenel, E., Shah, A., Paessens, A., Ruoff, H. J., von Briesen, H., … Wainberg, M. A. (1999). Resistance mutations selected in vivo under therapy with anti-HIV drug HBY 097 differ from resistance pattern selected in vitro. *Antiviral Research*, *42*(1), 15–24. doi:10.1016/S0166-3542(99)00010-8

Salehi, B., Kumar, N., Şener, B., Sharifi-Rad, M., Kılıç, M., Mahady, G., … Sharifi-Rad, J. (2018). Medicinal plants used in the treatment of human immunodeficiency virus. *International Journal of Molecular Sciences*, *19*(5), 1459. doi:ARTN 1459 doi:10.3390/ijms19051459

Sancho, R., Márquez, N., Gómez-Gonzalo, M., Calzado, M. A., Bettoni, G., Coiras, M. T., … Muñoz, E. (2004). Imperatorin inhibits HIV-1 replication through an Sp1-dependent pathway. *Journal of Biological Chemistry*, *279*(36), 37349–37359. doi:10.1074/jbc.M401993200

Santos, L. H., Ferreira, R. S., & Caffarena, E. R. (2015). Computational drug design strategies applied to the modelling of human immunodeficiency virus-1 reverse transcriptase inhibitors. *Memórias Do Instituto Oswaldo Cruz*, *110*(7), 847–864. doi:10.1590/0074-02760150239

Sarafianos, S. G., Das, K., Hughes, S. H., & Arnold, E. (2004). Taking aim at a moving target: Designing drugs to inhibit drug-resistant HIV-1 reverse transcriptases. *Current Opinion in Structural Biology*, *14*(6), 716–730. doi:10.1016/j.sbi.2004.10.013

Seckler, J. M., Leioatts, N., Miao, H., & Grossfield, A. (2013). The interplay of structure and dynamics: Insights from a survey of HIV-1 reverse transcriptase crystal structures. *Proteins: Structure, Function, and Bioinformatics*, *81*(10), 1792–1801. doi:10.1002/prot.24325

Shafer, R. W., & Schapiro, J. M. (2008). HIV-1 drug resistance mutations: An updated framework for the second decade of HAART. *AIDS Review*, *10*(2), 67–84.

Shafer, R. W., & Vuitton, D. A. (1999). Highly active antiretroviral therapy (HAART) for the treatment of infection with human immunodeficiency virus type 1. *Biomedicine & Pharmacotherapy*, *53*(2), 73–86. doi:10.1016/S0753-3322(99)80063-8

Shode, F. O., Mahomed, A. S., & Rogers, C. B. (2002). Typhaphthalide and typharin, two phenolic compounds from *Typha capensis*. *Phytochemistry*, *61*(8), 955–957. doi:10.1016/S0031-9422(02)00439-9

Singh, I. P., Bharate, S. B., & Bhutani, K. (2005). Anti-HIV natural products. *Current Science*, *89*(2), 269.

Sluis-Cremer, N. (2014). The emerging profile of cross-resistance among the nonnucleoside HIV-1 reverse transcriptase inhibitors. *Viruses*, *6*(8), 2960–2973. doi:10.3390/v6082960

Sluis-Cremer, N. (2018). Future of nonnucleoside reverse transcriptase inhibitors. *Proceedings of the National Academy of Sciences*, *115*(4), 637–638. doi:10.1073/pnas.1720975115

Sluis-Cremer, N., & Tachedjian, G. (2008). Mechanisms of inhibition of HIV replication by non-nucleoside reverse transcriptase inhibitors. *Virus Research*, *134*(1–2), 147–156. doi:10.1016/j.virusres.2008.01.002

Squires, K. E. (2001). An introduction to nucleoside and nucleotide analogues. *Antiviral Therapy*, *6*(Suppl. 3), 1–14.

Su, B.-N., Cuendet, M., Hawthorne, M. E., Kardono, L. B. S., Riswan, S., Fong, H. H. S., … Kinghorn, A. D. (2002). Constituents of the bark and twigs of *Artocarpus dadah* with cyclooxygenase inhibitory activity. *Journal of Natural Products*, *65*(2), 163–169. doi:10.1021/np010451c

Temiz, N. A., & Bahar, I. (2002). Inhibitor binding alters the directions of domain motions in HIV-1 reverse transcriptase. *Proteins: Structure, Function, and Genetics*, *49*(1), 61–70. doi:10.1002/prot.10183

Vanommeslaeghe, K., Hatcher, E., Acharya, C., Kundu, S., Zhong, S., Shim, J., … Mackerell, A. D. Jr. (2010). CHARMM general force field: A force field for drug-like molecules compatible with the CHARMM all-atom additive biological force fields. *Journal of Computational Chemistry*, *31*(4), 671–690. doi:10.1002/jcc.21367

Wensing, A. M., Calvez, V., Günthard, H. F., Johnson, V. A., Paredes, R., Pillay, D., … Richman, D. D. (2015). 2015 Update of the drug resistance mutations in HIV-1. *Topics in Antiviral Medicine*, *23*(4), 132–141.

Wensing, A. M., Calvez, V., Günthard, H. F., Johnson, V. A., Paredes, R., Pillay, D., … Richman, D. D. (2017). 2017 Update of the drug resistance mutations in HIV-1. *Topic in Antiviral Medicine*, *24*(4), 132–133.

Yin, J., Kouda, K., Tezuka, Y., Le Tran, Q., Miyahara, T., Chen, Y., & Kadota, S. (2004). New diarylheptanoids from the rhizomes of *Dioscorea spongiosa* and their antiosteoporotic activity. *Planta Medica*, *70*(1), 54–58. doi:10.1055/s-2004-815456

Zakaryan, H., Arabyan, E., Oo, A., & Zandi, K. (2017). Flavonoids: Promising natural compounds against viral infections. *Archives of Virology*, *162*(9), 2539–2551. doi:10.1007/s00705-017-3417-y

Zhan, P., Chen, X., Li, D., Fang, Z., De Clercq, E., & Liu, X. (2013). HIV-1 NNRTIs: Structural diversity, pharmacophore similarity, and implications for drug design. *Medicinal Research Reviews*, *33*(Suppl. 1), E1–E72. doi:10.1002/med.20241

Zhan, P., Pannecouque, C., De Clercq, E., & Liu, X. (2016). Anti-HIV drug discovery and development: Current innovations and future trends. *Journal of Medicinal Chemistry*, *59*(7), 2849–2878. doi:10.1021/acs.jmedchem.5b00497

Zhang, L., Xu, L., Xiao, S.-S., Liao, Q.-F., Li, Q., Liang, J., … Bi, K.-S. (2007). Characterization of flavonoids in the extract of *Sophora flavescens* Ait. by high-performance liquid chromatography coupled with diode-array detector and electrospray ionization mass spectrometry. *Journal of Pharmaceutical and Biomedical Analysis*, *44*(5), 1019–1028. doi:10.1016/j.jpba.2007.04.019

Zheng, G. Q., Ho, D. K., Elder, P. J., Stephens, R. E., Cottrell, C. E., & Cassady, J. M. (1994). Ohioensins and pallidisetins: Novel cytotoxic agents from the moss *Polytrichum pallidisetum*. *Journal of Natural Products*, *57*(1), 32–41. doi:10.1021/np50103a005

Zhou, P., Takaishi, Y., Duan, H., Chen, B., Honda, G., Itoh, M., … Lee, K. H. (2000). Coumarins and bicoumarin from *Ferula sumbul*: Anti-HIV activity and inhibition of cytokine release. *Phytochemistry*, *53*(6), 689–697.

Zhou, Y., Ning, Z., Lee, Y., Hambly, B. D., & McLachlan, C. S. (2016). Shortened leukocyte telomere length in type 2 diabetes mellitus: Genetic polymorphisms in mitochondrial uncoupling proteins and telomeric pathways. *Clinical and Translational Medicine*, *5*(1), 8. doi:10.1186/s40169-016-0089-2